



Different contributions of microbial and plant residues to soil organic carbon accumulation during planted forest and abandoned farmland restoration, Loess Plateau, China

Hongjian Hao · Rong Wang · Shicai Li · Duo Pian · Ning Peng · Ahejiang Sailike · Zhouchang Yu · Jiayi Shi · Xingbo Wang · Zihan Wang · Wei Zhang

Received: 18 March 2024 / Accepted: 23 May 2024
© The Author(s), under exclusive licence to Springer Nature Switzerland AG 2024

Abstract

Aims Plant and microbial residues are the primary drivers mediating soil organic carbon (SOC) accumulation in terrestrial ecosystems. However, how plant residues and microbial residues affect SOC accumulation and the underlying mechanisms remain poorly understood, especially in the succession process of different vegetation types.

Methods In this study, grasslands (GL) and *Robinia pseudoacacia* plantations (RP) restored for 10,

20, 30, and 40 years were used as research subjects on the Loess Plateau, and farmland was used as a control. Several indicators of soil physicochemical and plant characteristics, enzyme activity, amino sugar, lignin phenols were measured.

Results The results indicated that the contents of microbial and plant residue carbon in GL and RP increased with the increasing restoration years. However, the contribution of plant residue carbon to the SOC in GL and RP gradually decreased, while microbial residue carbon showed the opposite trend. In contrast, microbial residues were the main contributor to SOC in GL (62.8–75.1%), while plant residues were the main contributor to SOC in RP (47.2–58.3%). There was a difference in the bacterial and fungal residue carbon contribution to SOC between GL and RP. In GL, the dominant contributor to SOC changed from bacterial (47.7–37.2%) to fungal residues (15.1–37.9%). But in RP, it has always been dominated by fungal residue carbon (17.4–33.3%).

Conclusions More SOC accumulated in GL and RP in the form of microbial and plant residue carbon, respectively. In GL and RP, the contribution of carbon from fungal residues increased with the increase of recovery years. Overall, our research not only contributes to understanding the complexity of the carbon cycle in ecosystems, but also provides a valuable scientific basis for the management of soil carbon pools in different vegetation types under climate change.

Responsible Editor: Eric Paterson.

Supplementary Information The online version contains supplementary material available at <https://doi.org/10.1007/s11104-024-06772-x>.

H. Hao · R. Wang · S. Li · D. Pian · A. Sailike · Z. Yu · J. Shi · X. Wang · Z. Wang · W. Zhang
College of Grassland Agriculture, Northwest A&F University, Yangling 712100, Shaanxi, China

D. Pian
Institute of Pratacultural Science, Tibet Academy of Agriculture and Animal Husandry Science, Lhasa 850000, China

N. Peng
College of Life Sciences, Northwest A&F University, Yangling 712100, Shaanxi, China

W. Zhang (✉)
Shaanxi Engineering Research Center of Circular Agriculture, Yangling 712100, Shaanxi, China
e-mail: zwgwyd@163.com

Keywords Soil organic carbon · Plant residue · Microbial residue · Ratio of bacteria residue to fungal residue · Vegetation restoration

Introduction

As the largest carbon pool in terrestrial ecosystems, soil organic carbon (SOC) pool is approximately three and four times that of carbon the atmosphere and vegetation, respectively (Wang et al. 2022a). Consequently, a minor change in SOC storage can lead to considerable variations in atmospheric carbon dioxide concentration and ecosystem carbon balance (Tian et al. 2022), which will exacerbate or mitigate climate change (Voosen 2022). In recent decades, more and more studies have focused on SOC conversion and accumulation in terrestrial ecosystems because of the growing need to disentangle the soil carbon cycle and its effects on climate change (Hao et al. 2023; Medeiros et al. 2023). Emerging study has found that plant and microbial residues account for 19–42% and 40–59% of the terrestrial carbon pool, respectively (Chen et al. 2021), which together determine the storage of SOC (Liang et al. 2019; He et al. 2022). Microorganisms play a crucial role in regulating plant residues and microbial residues. On the one hand, they decompose plant residues by secreting extracellular enzymes (Liang and Zhu 2021), and on the other hand, form microbial residue carbon through anabolic metabolism (Xiao et al. 2023), both will lead to changes in the contribution of plant residues and microbial residues to SOC, affecting the sequestration of SOC pools (Xue et al. 2023; Zhang et al. 2023a). Therefore, a deeper understanding of relative contribution of carbon from plant and microbial residues to SOC pools and their trends is essential to elucidate the stabilization mechanisms of SOC and understanding the dynamics of the soil carbon pools under climate change.

Due to the varying decomposition rates of shoot and root litter from different vegetation types; microbial biomass, community composition, and enzyme activity are ultimately affected by the plants present (Qian et al. 2023). This leads to different contributions of microbial and plant residue carbon to the accumulation of SOC. For example, the formation of SOC in grasslands (GL) was accumulated mainly through the sequestration effect of microbial residues

(Ma et al. 2018). This is because the root exudates and dead roots in GL can be preferentially consumed by microorganisms (Roth et al. 2019), which promotes the formation of microbial residues. The relative oxygen restriction in forest soils can reduce microbial activity compared to GL, resulting in slower lignin decomposition (Charles et al. 2020; Qin et al. 2024). In consequence, the formation of SOC was accumulated primarily through the physical transfer of carbon from plant residues (such as lignin) in forest ecosystems (Wang et al. 2021). In addition, the contribution of plant residues and microbial residues to SOC is not static and will exhibit varying trends with the increasing restoration years. For example, previous research has found that the accumulation of SOC changes from being dominated by plant residues to being dominated by microbial residues with the increasing restoration years (Yang et al. 2022a). In summary, the pathways by which plant and microbial residues regulate the accumulation of soil carbon pools are not yet clear because of the wide variations in study areas, study subjects, and restoration chronosequences. Therefore, further research is needed to verify the driving role of microbial and plant residues in formation of soil carbon pools.

With widespread academic recognition of amino sugars as microbial residue markers (Zhang and Amelung 1996), an increasing number of studies have focused on the relative contribution of bacterial and fungal residues to SOC (Tian et al. 2022; Xu et al. 2022; Zhang et al. 2023b). However, relevant studies on the contribution of fungal and bacterial residues to SOC have not reached consistent conclusions. For instance, it has been noted that bacterial residues are the main contributors to SOC in farmland and grassland (Li et al. 2024b; Yang et al. 2022b), while another study concluded the contribution of fungal residues to SOC surpassed that of bacterial residues in forests (Tian et al. 2022). Meanwhile, a global-scale study also demonstrated that the contribution of bacterial and fungal residues to soil organic carbon (SOC) differs between various ecosystems (Wang et al. 2021). One reason for such differences may be due to diversity in the growth, reproduction, and physiological characteristics of fungi and bacteria (Arcidicono et al. 2023; Xiang et al. 2018). Another more important reason is that fungi and bacteria also differ in the type of substrate and the soil environment

they inhabit (Beidler et al. 2020), which will affect fungal and bacterial growth, and affect the accumulation of SOC (Feng et al. 2023). Interestingly, our previous studies found that the substrate quality and soil environments change under different vegetation types and restoration years (Cao et al. 2023; Sun et al. 2023; Zhang et al. 2019), but whether this change affects the contribution of bacterial and fungal residues to SOC accumulation remains poorly understood. Therefore, it is necessary to incorporate different vegetation types as well as restoration years in the study, which will help us accurately understand the contribution of fungal and bacterial residues in the process of SOC accumulation, and fill the knowledge gaps on the mechanism of SOC accumulation during the vegetation restoration.

The ecological environment of the Loess Plateau is relatively fragile, and soil erosion is severe (Xu et al. 2019; Ye et al. 2022). In recent decades, with the continuous implementation of ecological restoration projects, the region has achieved positive results in vegetation restoration, with a substantial increase in vegetation cover (Tian et al. 2024; Zhang et al. 2022), and a substantial increase in ecosystem carbon sequestration potential (Wang et al. 2024; Yang et al. 2023). This has provided a key focus for research on soil carbon sequestration and ecological restoration. To date, research on SOC in ecological restoration of the Loess Plateau has mainly focused on estimating soil carbon storage and the content and dynamics of soil carbon pools (Ghani et al. 2023; Yuan et al. 2023; Zeng et al. 2022). As the primary contributors to the soil carbon pool, the relative contributions of plant and microbial residues to SOC accumulation, and the reasons for the differences, have not been thoroughly studied in the Loess Plateau. Thus, in this study, GL and *Robinia pseudoacacia* plantations (RP) restored for 10, 20, 30, and 40 years were used as research subjects, and three hypotheses were described: (1) With the increasing restoration years, the carbon content of microbial and plant residues in each vegetation type increased significantly; (2) Microbial residue carbon is the main contributor to SOC in GL, while plant residue carbon is the main contributors in RP; (3) In GL and RP restorations, the contribution of fungal residues will increase, and bacterial residue contributions decrease, over time.

Materials and methods

Study area

The study was conducted at the Wuliwan Watershed in Ansai District, Yan'an City, Shaanxi Province, China (109°19'-109°22'E, 36°51'-36°52'N), with an altitude of 1060–1400 m above sea level. This area has semi-arid monsoon climate and the annual mean precipitation is approximately 500 mm. The annual mean temperature and annual mean frost-free period approximately 8.8 °C and 160 d. To improve the environment in this area, Chinese government implemented the Grain for Green Project in 1999. The vegetation cover increased significantly, grasslands and plantations with different restoration years were formed, accounting for 36.9% and 31.3% of the Wuliwan Watershed, respectively (Fig. S1, Zhang et al. 2019). Among which the dominant species of grassland were *Roegneria kamoji*, *Stipa bungeana*, *Artemisia sacrorum*, and *Lespedeza davurica*, and the dominant species of plantations was *Robinia pseudoacacia*. This provides an ideal template for an in-depth understanding of the theoretical studies on vegetation restoration in Loess hilly areas.

Experimental design and sample collection

The study began in August 2022. After reviewing documents from local government departments, visiting local farmers, and combining field surveys, we selected three typical vegetation types (RP and GL) which had both been restored for four age classes (10, 20, 30, and 40 years) in the Wuliwan Watershed as the research objects for our study. We chose farmlands (FL) as the control because both vegetation types were FL before restoration. Same as the control FL, the GL and RP were in maize (*Zea mays L.*) and millet (*Setaria italica*) rotation before restoration, and nitrogen and phosphorus fertilizers were applied annually in spring at rates of 43 kg ha⁻¹ and 28 kg ha⁻¹, respectively. Each of the vegetation types with different restoration year (GL10, GL20, GL30, GL40, and RP10, RP20, RP30, RP40) and the FL were independently replicated three times, total 12 GL stands, 12 RP stands, and three FL stands were selected. The geographical features of the selected stands were similar, such as soil classification, elevation, slope,

and slope aspect (Table S1). Three independent plots (20 m × 20 m) were set up at each stand, which were convenient for follow-up sampling and index determination, and data were collected from 81 plots (three replicates × 27 stands).

After removing the debris, roots, plant residues, and litter from the soil surface, sampling was performed using the “S” sampling method, using a soil auger which has 9 cm in diameter, to collect 10 soil cores within each plot and mix into a single soil sample. The collected soil samples were passed through a 2 mm mesh and then divided into two parts, one was stored at 4 °C before the determination of microbial biomass, one was air-dried and stored at room temperature (25 °C) to determine physicochemical properties of the soil, such as pH and soil water content. In each sampling plot, we collected one soil sample using a ring knife to determine the soil bulk density. We randomly selected 20 RP trees for leaf sampling in each plot. Healthy mature leaves were collected from the upper, middle, and lower parts of the tree canopy from four directions, that is, east, west, south, and north. Leaves in the well-mixed uniform standard samples were recorded as the aboveground biomass of the RP. Five 1 m × 1 m subplots within each plot were selected using the five-spot-sampling method. The aboveground biomass of the herbaceous plants in the subplots was recorded as the aboveground biomass of the GL. After removing the aboveground plants in GL and RP plots, the roots were excavated at a depth of 0–50 cm in each plot and brought back to the laboratory as the fine root biomass. The aboveground plants and fine roots were washed and dried at 75 °C to constant weight, and then the aboveground and fine roots were calculated. Three litter collectors with 5 m × 5 m in RP, while 1 m × 1 m in GL were randomly set up to collect litter, in each plot. Then mixed litter material was collected from the same plot and brought back to the laboratory, dried at 75 °C to constant weight as litter biomass, and crushed for determination of carbon and nitrogen contents.

Laboratory analysis

Soil physicochemical and plant characteristics analyses

Taking the ratio of 1:5 soil to water as the standard, a portable pH meter (STARTER 300, OHAUS, USA)

was used to determine the soil pH. The soil water content was determined using the weighing method after being dried to a constant weight of 105 °C. We used the cutting ring method to determine soil bulk density (Deng et al. 2014). A laser particle-size analyzer was used to determine the soil clay content (Mastersizer, 2000; Malvern Instruments, Malvern, UK). After leaching with 0.05 mol·L⁻¹K₂SO₄ (soil–liquid ratio 1:5), a total organic carbon analyzer was used to determine the dissolved organic carbon and dissolved organic nitrogen (Liqui TOC II, Elementar, Germany). SOC was determined by an elemental analyzer (Elementar, Vario Max CN, Germany). Microbial biomass carbon and nitrogen were determined by chloroform fumigation leaching method (Li et al. 2021a).

The carbon contents of fine root, litter, and plant were determined using the acid hydrolysis-K₂Cr₂O₇ oxidation method, while nitrogen contents of fine root, litter, and plant were determined using H₂SO₄-H₂O₂ and K₂SO₄, and CuSO₄·5H₂O as mixed catalysts, and then determined using an AA3 continuous flow analyzer.

Soil enzyme activity determination

The activities of soil oxidase and hydrolase were determined by DeForest's (2009) and Saiya-Cork's et al. methods (2002), respectively. The phenol oxidase and catalase substrates were synthesized by a 1:2 mixture of L dihydroxyphenylalanine and EDTA-3Na, 4-MUB-β-D-cellobioside and 4-MUB-β-D-glucopyranoside were cellobiohydrolase and β-1,4-xylosidase substrates, respectively. After the incubation, the fluorescence value was detected by a multifunctional microplate reader (Tecan Infinite M200, Austria). Excitation at 365 nm and fluorescence determination at 460 nm (oxidase) and 450 nm (hydrolase) wavelengths were performed.

Soil amino sugar assessment

Soil amino sugars were extracted using Joergensen's method (Joergensen 2018). The amino sugar extract was analyzed using gas chromatography (GC, Agilent Technologies, USA). 1 μL of amino sugar extract was injected into the chromatographic for assay. The gas chromatography inlet temperature was set at 250 °C, the split ratio was 30:1, and N₂ was used as the carrier

gas at a flow rate of $0.6 \text{ mL} \cdot \text{min}^{-1}$. Soil amino sugars were separated according to the peak times of the three amino sugars in the standard sample. The calculation was as follows (Liang et al. 2019):

$$\text{MRC}_F = \left(\frac{\text{GlcN}(\text{mg} \cdot \text{kg}^{-1})}{179.2} - \frac{2 \times \text{MurA}(\text{mg} \cdot \text{kg}^{-1})}{251.2} \right) \times 179.2 \times 9 \quad (1)$$

$$\text{MRC}_B = 45 \times \text{MurA}(\text{mg} \cdot \text{kg}^{-1}) \quad (2)$$

$$\text{MRC} = \text{MRC}_F + \text{MRC}_B \quad (3)$$

where the molecular weights of GlcN and MurA were 179.2 and 251.2, respectively. The conversion factor of fungal GlcN to fungal residue carbon was 9 and the conversion factor of bacterial MurA to bacterial residue carbon was 45. The contribution of microbial (fungal and bacterial) residues to SOC = $(\text{MRC}_F + \text{MRC}_B)/\text{SOC}$.

Determination of lignin phenols

Lignin phenol content was determined according to the methods of Hedges and Ertel method (Hedges and Ertel 1982). Lignin phenols were calculated by adding cinnamyl-type monomers (C), syringyl-(S), and vanillyl-(V).

$$P = \frac{\left(\frac{V}{33.3\%} + \frac{S}{90\%} + C \right)}{3\% \times \text{SOC}} \times 100\% \quad (4)$$

where C, S, and V denote the carbon contents related to C-, S-, and V-type phenols ($\text{g} \cdot \text{kg}^{-1}$), respectively, and 3% denotes the minimal lignin content of the principal plant residues.

Statistical analyses

Statistical tests were performed using SPSS 22 software (IBM SPSS Statistics, USA). The distribution of all data was performed using the Shapiro-Wilk test, and the results were normally distributed. Two-way analysis of variance was used to explore the effects of different vegetation types and restoration years excluding FL on vegetation and soil physicochemical properties. Duncan's method was used to test the significance of the differences, and the significance

level was $P < 0.05$. The relationship between vegetation properties, soil physicochemical properties, and enzyme activity was explained by using Spearman analysis and Mantel test in R statistical software (version 4.2.2). Redundancy analysis was performed using the CANOCO 5 software to determine the relationship between plant residue carbon and microbial (fungal and bacterial) residue carbon and their contribution to vegetation and soil physicochemical properties. Using SmartPLS3 software, based on the effects of soil and plant factors on plant residue carbon and microbial (fungal and bacterial) residue carbon, a partial least squares path model was established (model requirements SRMR < 0.2 , NFI > 0.9). Origin 2022 was used for graphing.

Results

Vegetation characteristics and soil properties with the progression of vegetation restoration

In GL, cover, aboveground biomass, the carbon content of plant, fine root, and litter increased significantly during the recovery years. Fine root nitrogen content first increased before decreasing, and the maximum and minimum values appeared in 30-Y and 10-Y, respectively ($P < 0.05$, Table 1, Table S2). In RP, cover first increased and then decreased. The peak occurred at 30-Y and the nadir occurred at 10-Y. Aboveground biomass first decreased and then increased. Fine root nitrogen content significantly decreased, and litter carbon content showed the opposite trend ($P < 0.05$). Litter nitrogen content showed a trend of decreasing initially and then stabilized.

As shown in Table 2, pH and bulk density in FL were significantly higher than GL and RP, respectively, 2.5–7.9% and 3.9–11.1% (pH); 4.6–15.3% and 5.3–19.1% (bulk density). But soil water content and clay content were significantly lower than those of GL and RP ($P < 0.05$). With the increase of the recovery years, the soil water content was $\text{FL} < \text{GL} < \text{RP}$ (except for the 40-Y). Furthermore, the pH and bulk density in GL and RP continued to decrease, with a reduction of 5.5% and 11.2% in GL, 7.5% and 14.5% in RP. The clay content first increased, then stabilized, and finally increased. Microbial biomass carbon and nitrogen were generally manifested as $\text{RP} > \text{GL} > \text{FL}$.

Table 1 Changes of plant factors with different sampling stands

Stands	cover (%)	AB (g·m ⁻²)	FRB (g·m ⁻²)	LB (g·m ⁻²)	PC (g·kg ⁻¹)	PN (g·kg ⁻¹)	PC/PN	FRC (g·kg ⁻¹)	FRN (g·kg ⁻¹)	FRC/FRN	LC (g·kg ⁻¹)	LN (g·kg ⁻¹)	LC/LN
GL10	45.0±1.53Bd	131.6±7.09Bd	155.9±3.45Ad	52.5±4.29Bd	362.1±7.30Bd	12.4±0.94Bd	29.6±1.84Aa	323.7±5.89Bd	10.1±0.37Bd	32.0±0.70Aa	295.8±7.39Bd	12.3±0.22Ba	24.0±0.55Ac
GL20	55.0±2.08Bc	196.2±9.71Ac	187.6±5.61Ac	85.1±6.03Bc	399.2±8.18Bc	16.3±0.54Bc	24.6±1.02Ab	367.7±8.44Bc	14.4±0.57Bc	25.5±0.84Ab	339.5±5.26Bc	13.1±0.36Ba	25.9±0.70Ac
GL30	72.7±1.45Bb	290.6±5.42Ab	233.2±6.31Ab	122.8±4.41Bb	436.1±7.64Bb	25.2±1.09Aa	17.4±1.07Ac	405.2±9.07Ab	21.1±0.63Aa	19.2±0.149Bc	377.9±5.69Ab	13.2±0.47Ba	28.7±0.59Ab
GL40	62.7±1.45Ba	345.4±8.08Aa	282.3±5.83Aa	175.9±5.08Ba	461.5±4.84Aa	21.3±0.30Bb	21.7±0.53Ab	439.0±5.71Aa	16.9±0.68Ab	26.1±1.39Ab	410.5±6.52Aa	13.2±0.26Ba	31.1±0.82Aa
RP10	54.7±2.40Ac	196.1±8.09Aa	109.4±8.48Bc	219.1±4.97Ad	463.2±6.12Aa	25.8±0.73Ac	18.0±0.28Ba	424.2±6.72Aa	21.5±0.54Aa	19.7±0.48Bc	365.5±3.79Ab	18.2±0.48Aa	20.1±0.68Bc
RP20	68.3±3.33Ab	175.5±6.65Aa	163.5±6.41Bb	339.0±9.08Ac	439.2±9.60Aa	28.8±0.73Abc	15.3±0.71Bb	417.1±5.08Aa	19.7±0.38Ab	21.2±0.23Bbc	362.2±5.39Ab	16.0±0.46Ab	22.7±0.44Bb
RP30	84.3±2.33Aa	142.9±7.58Bb	196.2±7.06Ba	492.1±6.87Ab	462.9±4.57Aa	36.9±1.25Aa	12.6±0.31Bc	434.6±5.90Aa	19.6±0.57Ab	22.2±0.68Aab	384.8±7.49Aab	16.0±0.30Ab	24.0±0.036Aab
RP40	72.3±1.45Ab	174.7±7.20Ba	214.4±6.41Ba	565.1±6.94Aa	444.8±6.34Aa	30.9±0.68Ab	14.4±0.50Bb	426.4±5.08Aa	18.0±0.26Ac	23.7±0.15Aa	390.9±8.20Aa	15.5±0.14Ab	25.2±0.37Ba

The GL and RP characterize the different selected vegetation restoration types, which means grassland and *Robinia pseudoacacia* plantations, respectively. The 10, 20, 30, and 40 means the four restoration years, including 10 years, 20 years, 30 years, and 40 years, respectively. AB: aboveground biomass, FRB: fine root biomass, LB: litter biomass, PC: plant carbon, PN: plant nitrogen, PC/PN: plant carbon–nitrogen ratio, FRC: fine root carbon, FRN: fine root nitrogen, FRC/FRN: fine root carbon–nitrogen ratio, LC: litter carbon, LN: litter nitrogen, LC/LN: litter carbon–nitrogen ratio. Different normal and bold lowercases signify the significant difference at 0.05 level ($P < 0.05$) among different restoration years of the GL and RP, respectively. Values are means ± standard errors ($n = 3$). Capital letters signify that the GL and RP had significant differences at 0.05 level ($P < 0.05$) under the same restoration year

Table 2 Changes of soil abiotic and biotic factors with different sampling stands

Stands	pH	BD (g·cm ⁻³)	SWC (%)	clay (%)	DOC (mg·kg ⁻¹)	DON (mg·kg ⁻¹)	MBC (mg·kg ⁻¹)	MBC/MBN	MBN (mg·kg ⁻¹)	MBC/MBN
FL	8.73±0.07aa	1.31±0.01aa	10.70±0.20cd	14.48±0.32cd	20.95±0.68ee	7.27±0.26de	63.99±2.37ee	14.82±0.49ee	4.32±0.05de	4.88±0.07Ac
GL10	8.51±0.04Ab	1.25±0.01Ab	9.66±0.11Bc	18.54±0.40Ac	29.10±1.11Bd	8.82±0.17Bd	104.23±2.49Bd	21.39±0.61Bd	4.88±0.07Ac	4.95±0.07Ac
GL20	8.34±0.03Ac	1.24±0.01Ab	12.64±0.58Bb	21.31±0.33Ab	42.95±1.61Bc	11.56±0.55Bc	130.34±2.70Bc	26.3±0.37Bc	5.37±0.06Bb	5.79±0.13Ba
GL30	8.19±0.02Ad	1.19±0.01Ac	13.43±0.28Bb	20.60±0.59Ab	65.82±2.96Bb	15.79±0.37Bb	172.08±2.16Bb	32.08±0.10Bb	5.79±0.13Ba	4.75±0.06Ad
GL40	8.04±0.03Ac	1.11±0.02Ad	15.53±0.28Aa	23.36±0.35Aa	92.39±3.54Ba	18.73±0.85Ba	226.56±3.92Ba	39.16±0.75Ba	36.7±1.20Ad	5.31±0.04Ac
RP10	8.39±0.02Bb	1.24±0.01Ab	13.84±0.36Abc	18.19±0.19Ac	49.79±2.97Ad	13.30±0.68Ad	174.29±4.41Ad	26.29±4.70Ac	61.50±1.63Ab	6.45±0.11Aa
RP20	8.29±0.02Abc	1.18±0.01Bc	14.87±0.47Aab	20.13±0.36Bb	74.13±4.12Ac	17.61±1.06Ac	262.29±4.70Ac	49.43±0.80Ac	69.49±1.73Aa	6.45±0.11Aa
RP30	8.16±0.02Ac	1.17±0.02Ac	16.03±0.51Aa	21.10±0.20Ab	117.17±5.09Ab	23.27±1.39Ab	361.36±3.58Ab	61.50±1.63Ab	69.49±1.73Aa	6.45±0.11Aa
RP40	7.76±0.04Bd	1.06±0.02Ad	13.24±0.52Bc	22.48±0.68Aa	165.13±7.35Aa	28.76±1.03Aa	447.53±5.92Aa	69.49±1.73Aa	6.45±0.11Aa	6.45±0.11Aa

pH mean pH in the first 10 cm of soil, BD soil bulk density, SWC soil water content, clay the percentage of soil clay, DOC dissolved organic carbon, DON dissolved organic nitrogen, MBC microbial biomass carbon, MBN microbial biomass nitrogen, MBC/MBN microbial biomass carbon–nitrogen ratio. Different lowercases letters signify significant difference between FL and GL at different restoration years at 0.05 level ($P < 0.05$), and different bold lowercases letters signify significant difference between FL and RP at different restoration years at 0.05 level ($P < 0.05$). Values are means ± standard errors ($n = 3$). Capital letters signify that the GL and RP had significant differences at 0.05 level ($P < 0.05$) under the same restoration year. Treatment codes are the same as Table 1

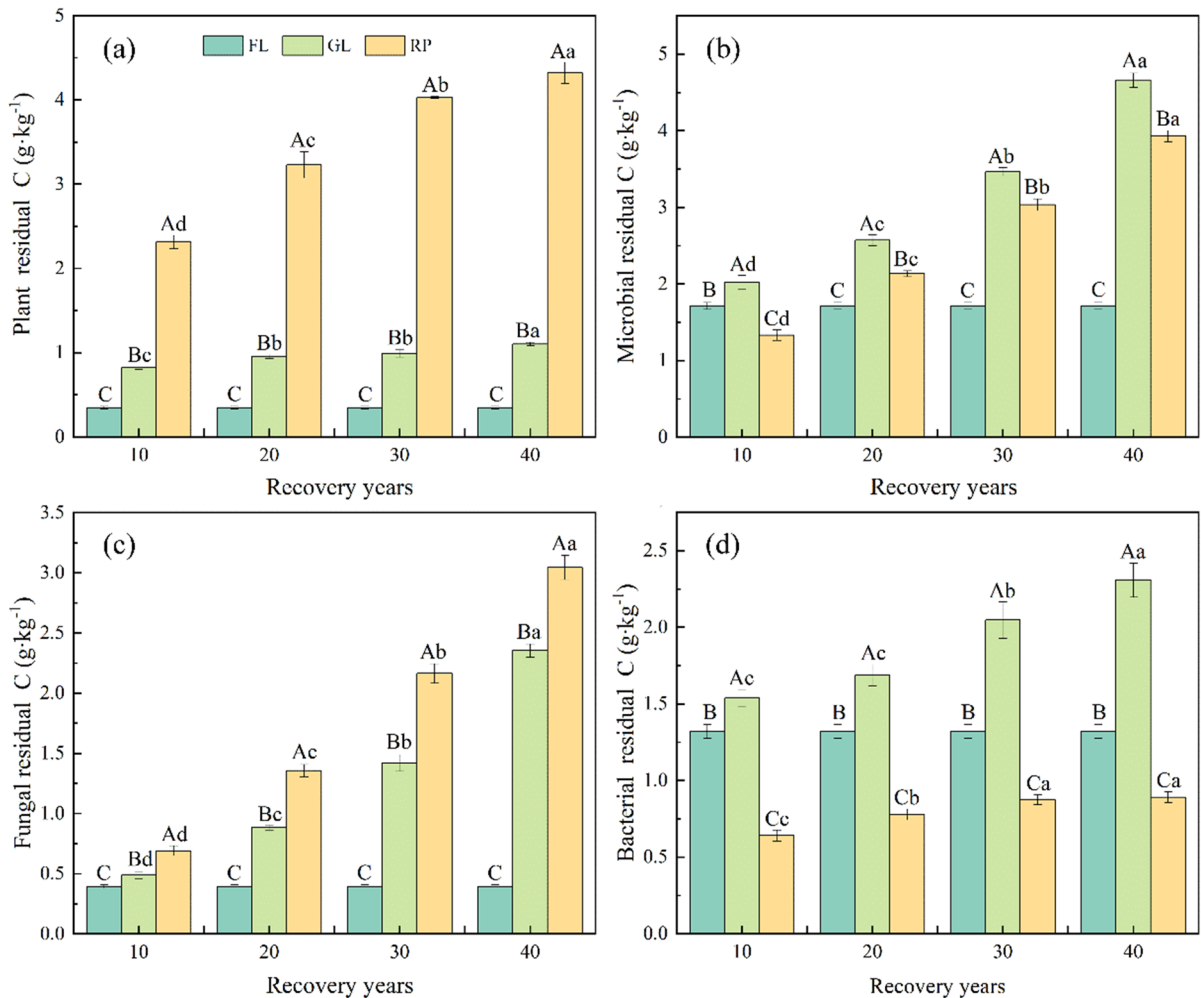


Fig. 1 Carbon content of different residues types with four restoration years under different vegetation types. Note: The FL, GL, and RP characterize the different selected vegetation restoration types, which means farmland, grassland, and *Robinia pseudoacacia* plantations, respectively. The 10, 20, 30, and 40 means the four restoration ages, including 10 years, 20

years, 30 years, and 40 years, respectively. Different capital letters signify the significant difference among different land-use types ($P < 0.05$) at the same restoration years. Different lower-cases signify significant difference among different restoration years ($P < 0.05$) at the same land-use types, respectively. The error bars are the standard errors

among different vegetation types, showed a growing trend in GL and RP.

Changes of residues carbon content in different vegetation restoration

In the same recovery year, plant residue carbon was significantly greater in GL and RP than in FL by 134.3–214.3% and 560.0–1134.3%, respectively (Fig. 1). It increased significantly during the recovery period in the GL and RP ($P < 0.05$). In contrast to the

plant residue carbon content, the microbial residue carbon content was generally $GL > RP > FL$, but in 10-Y, it was $GL > FL > RP$. With an increase in recovery years, the microbial residue carbon content in GL and RP increased. Fungal and bacterial residue carbon content in GL ranged between 0.5 and 2.4 g·kg⁻¹, 1.5 and 2.3 g·kg⁻¹, respectively. The proportion of fungal residue carbon increased from 24.1% (10-Y) to 50.5% (40-Y). Conversely, the proportion of bacterial residue carbon decreased from 76.1 to 49.5%. Fungal residue carbon content in RP increased from

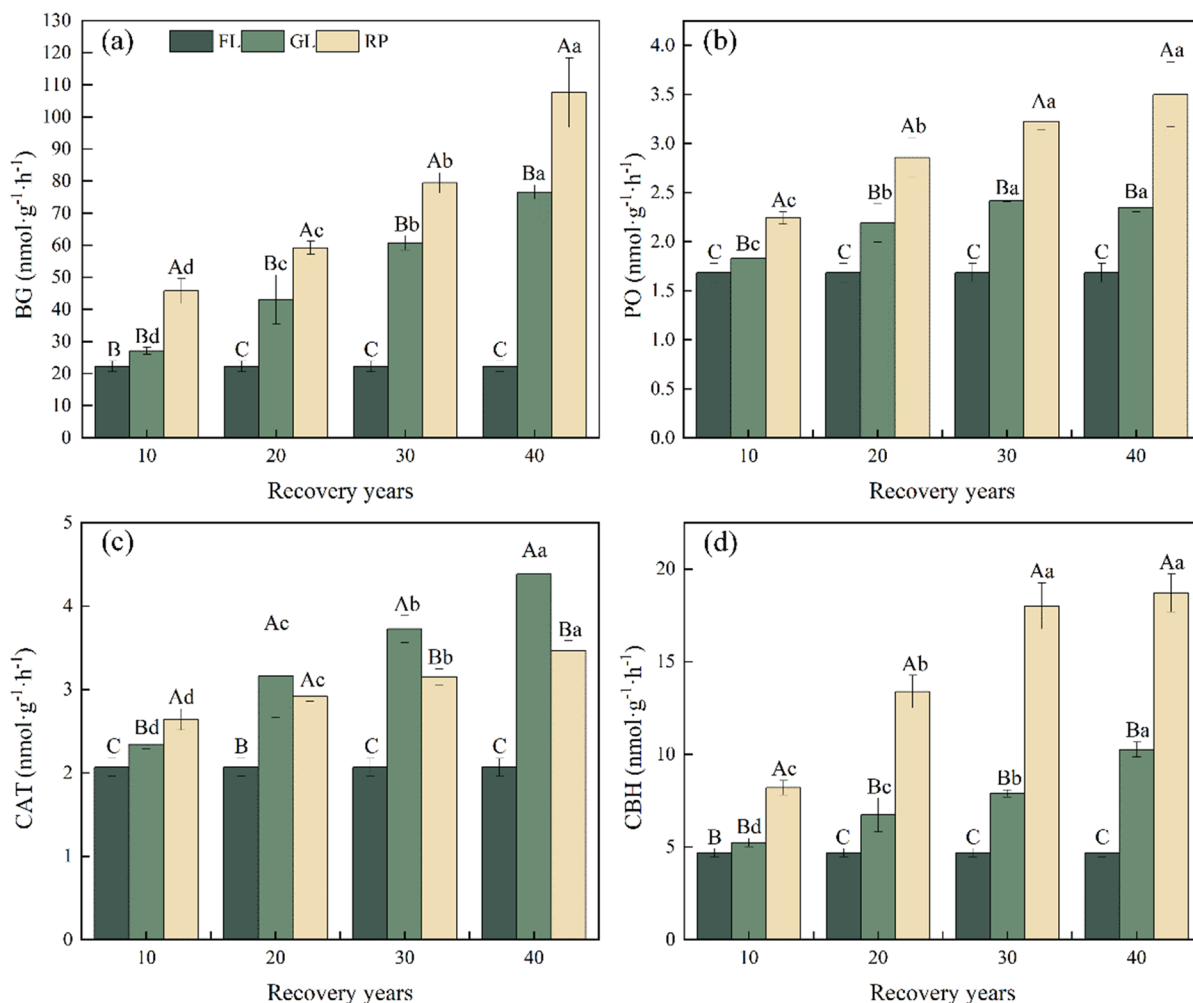


Fig. 2 Soil enzyme activity with four restoration years under different vegetation types. Note: The BG, PO, CAT, and CBH means β -1,4-xylosidase, phenol oxidase, catalase, cellobiohy-

drolase, respectively. The error bars are the standard errors. Treatment codes are the same as Fig. 1

0.7 g·kg⁻¹ to 3.0 g·kg⁻¹, accounting for 51.9–77.4% of the carbon content of microbial residues. Bacterial residue carbon content ranged from 0.6 to 0.9 g·kg⁻¹, showing a trend of increasing first and then stabilizing, and the proportion of carbon in the microbial residues decreased from 47.9 to 22.6%.

Changes of enzyme activity in different vegetation restoration

There were statistical differences in soil carbon-degrading enzyme activities in GL and RP with different restoration years (Fig. 2). The activity of β -1,4-xylosidase, phenol oxidase, and

cellobiohydrolase were shown as GL > FL > RP, compared with FL, GL and RP increased by 0.2–2.4, 0.09–0.4, and 0.1–1.2 times (GL), 1.0–3.8, 0.3–1.1 and 0.7–3.0 times (RP), respectively. However, enzyme activity of catalase was shown as GL > RP > FL except for 10-Y. The activities of β -1,4-xylosidase, catalase, and cellobiohydrolase in the GL increased significantly with increasing recovery years ($P < 0.05$), while phenol oxidase activity showed a trend of increasing first and then stabilizing. The activities of catalase and β -1,4-xylosidase in RP increased significantly ($P < 0.05$), while the activities of phenol oxidase and cellobiohydrolase first increased and then stabilized, and

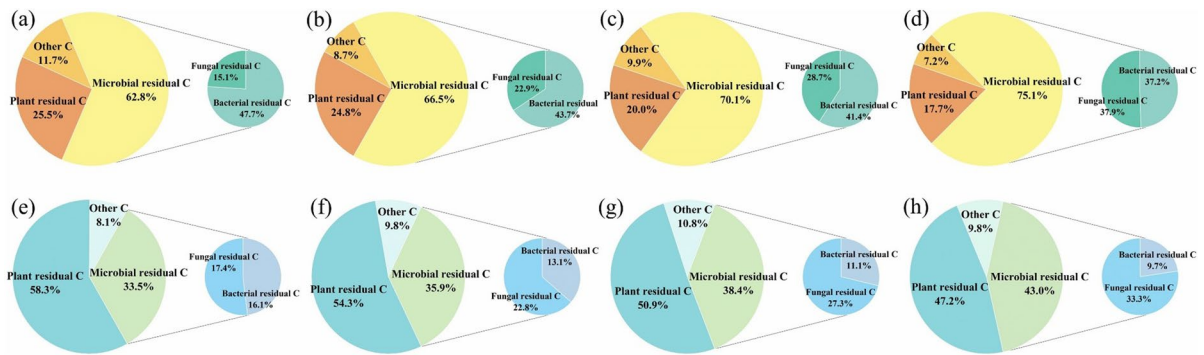


Fig. 3 Pie chart of contribution in plant, microbial, bacterial, and fungal residual carbon to soil organic carbon under four restoration years under different vegetation types. Note: The

vegetation type in (a), (b), (c) and (d) are grassland and the vegetation type in (e), (f), (g) and (h) are *Robinia acacia* plantations

from 10-Y to 30-Y increased by 0.36 and 0.56 times ($P < 0.05$), respectively.

Contribution of residue carbon to SOC

In RP, the contribution was 58.3% at 10-Y, which was markedly higher than that in other years ($P < 0.05$). With the increase in recovery years, the contribution of plant residue carbon to SOC exhibited a decreasing trend (Fig. 3). The recovery year significantly influenced the contribution of microbial, fungal, and bacterial residue carbon to the SOC content (Fig. 3). The contribution of bacterial residue carbon declined with the increase of recovery years (47.7–37.2%), while the contribution of fungal residue carbon increased (15.1–37.9%), which was ultimately manifested by an increase in the contribution of microbial residue carbon in GL (62.8–75.1%). While the contribution of microbial and fungal residue carbon in RP increased significantly compared with 10-Y and the contribution increased by 22.1% and 47.8% at 40-Y, respectively. The contribution of bacterial residue carbon was between 9.7 and 16.1%, and the trend decreased as the recovery year increased.

Effects of environment on carbon of plant and microbial residues

In Fig. 4, the enzyme activities of catalase, pH, clay, and fine root biomass were the best explanatory

variables for plant residue carbon. Microbial biomass carbon, microbial biomass nitrogen, and the activities of cellobiohydrolase and phenol oxidase were the most suitable explanatory variables for fungal residue carbon. Except for aboveground biomass and fine root biomass, the other vegetation characteristics, soil physicochemical properties, and enzyme activities were highly correlated with bacterial residue carbon. The Redundancy analysis results showed that SOC, STN, pH, litter biomass, and fine root biomass contributed the most to the residues (Fig. 5b, d, f, h). In GL, the carbon content of the bacterial residues was positively correlated with fine root biomass, total nitrogen content, and microbial biomass carbon–nitrogen ratio (Fig. 5c). A significant positive correlation existed between the carbon content of fungal residues and litter biomass, and litter carbon content. But of fungal residues carbon content was negatively correlated with pH and bulk density. Cover, soil water content, and clay content had the greatest effects on plant residue carbon (Fig. 5a). In the RP, cover had the greatest impact on the bacterial residue carbon content. Fungal residue carbon content was positively correlated with litter biomass and microbial biomass carbon–nitrogen ratio, and negatively correlated with pH and bulk density (Fig. 5e, g). fine root biomass and litter biomass had substantial effects on the plant residue carbon content, with a significant positive correlation (Fig. 5e, g).

In GL, fungal residue carbon was directly controlled by vegetation (litter biomass and litter carbon–nitrogen ratio), bacterial residue carbon content

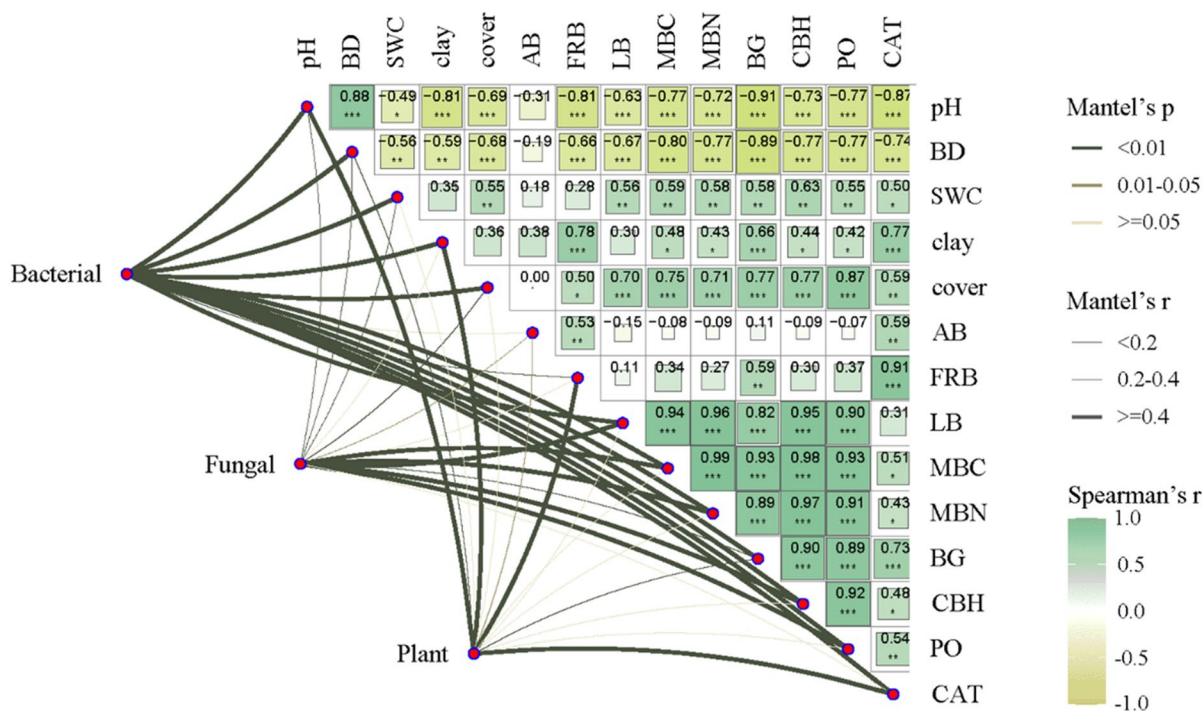


Fig. 4 Correlations between environmental variables and plant, fungal, and bacterial residue carbon. Note: Edge width corresponds to the Mantel's r statistics for the corresponding distance correlations, and edge color denotes the statistical significance. The positive and negative relationships between the two variables are represented by dark green and light green, respectively. The deeper the color, the stronger the relationship. ns indicates no significant difference; * indicates

$P < 0.05$; ** indicates $P < 0.01$; *** indicates $P < 0.001$. BD: soil bulk density, SWC: soil water content, AB: aboveground biomass, FRB: fine roots biomass, LB: litter biomass, MBC: microbial biomass carbon, MBN: microbial biomass nitrogen, BG: β -1,4-xylosidase enzyme activity, CBH: cellobiohydrolase enzyme activity, PO: phenol oxidase enzyme activity, CAT: catalase enzyme activity

was controlled by microbial biomass carbon–nitrogen ratio and vegetation, and pH indirectly affected fungal and bacterial residue carbon content through microbial biomass carbon–nitrogen ratio and vegetation (Fig. 6). In RP, fungal and plant residue carbon contents were controlled by microbial biomass carbon–nitrogen ratio and vegetation (litter biomass and litter carbon–nitrogen ratio), respectively. The pH indirectly affected fungal and plant residue carbon content by negatively affecting microbial biomass carbon–nitrogen ratio and vegetation. However, under different vegetation types, residue carbon affected SOC in different ways. In GL, the effect of residue carbon on SOC was significantly positively related with fungal and bacterial residue carbon content ($P < 0.05$), but plant residue carbon content was not significant. In RP, the effect of residual carbon on SOC was significantly positively correlated with

fungal and plant residual carbon content ($P < 0.05$), but the bacterial residual carbon content was not significant.

Discussion

Management affects accumulation of residues under different vegetation types

Vegetation restoration promotes the accumulation of carbon from microbial and plant residues (Fig. 1), which favors SOC formation (Hu and Lan 2020; Yang et al. 2022a). The contribution of microbial residues to organic carbon was the largest in FL and GL, while the SOC in RP was mainly dependent on plant residues (Table S4). Unlike GL and RP, FL was mowed after harvest each year, which reduced the input of

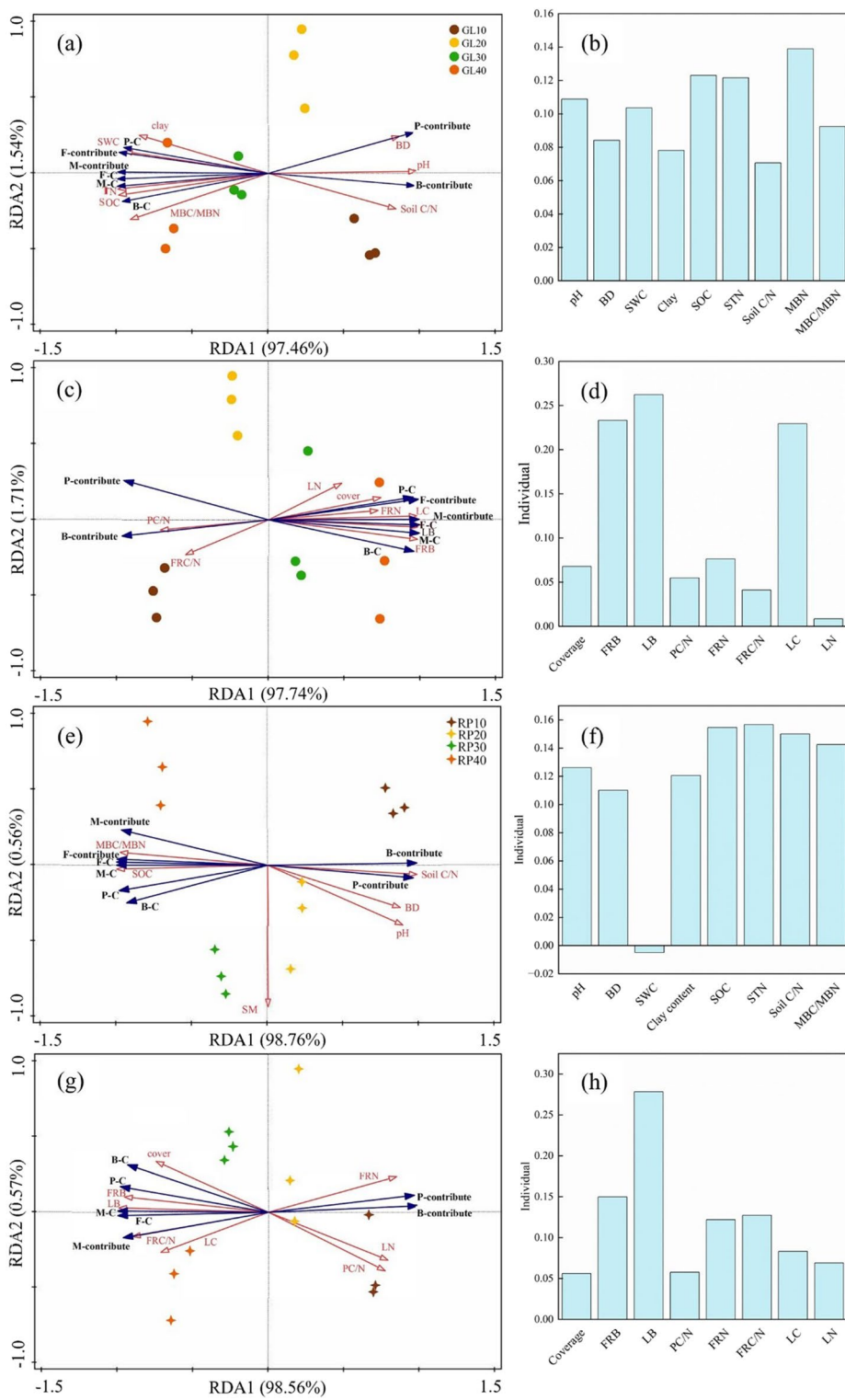
fresh lignin and directly affected the accumulation of carbon in plant residues (Li et al. 2023). The microbial residue carbon content in GL was significantly larger than that in RP, whereas the plant residue carbon content was significantly lower than that in RP (Fig. 1). The uneven distribution of aboveground and belowground biomass between GL and RP was a key reason for this difference (Table 1). GL has most of its biomass concentrated underground and has well-developed root systems and root exudates (Table 1). Nutrient-rich root exudates promote growth and increase the activity of soil microorganisms (Yang et al. 2022c), and microbial residues from metabolites increase with microbial biomass (Ding et al. 2020). This has resulted in higher levels of microbial residue carbon in the soil (Fig. 1). Soil microorganisms in the GL transformed plant carbon at a higher rate than those in RP (Wang et al. 2021). In contrast, RP, a woody plant, is rich in foliage and litter material, and aboveground biomass increases the carbon content of plant residues (Charles et al. 2020). Microbial residue carbon is more difficult to accumulate because of the presence of an organic layer in RP soils, in which microbial residues are less likely to be adsorbed by minerals and thus less likely to be conserved (Wang et al. 2021).

Tilling disturbs FL soil greatly, inhibits the formation of aggregates, destroys fungal mycelia, reduces the accumulation of carbon from fungal residues, and makes the contribution of carbon from bacterial residues dominant (Yang et al. 2022d; Zhou et al. 2023). In this study, we showed that among the microbial residue carbon in GL, the content of bacterial residue carbon contributed the most to SOC (37.2–47.7%) (Fig. 3). Soil pH made a difference to the structure of soil microbial communities, biomass, and diversity (Cheng et al. 2020; Zhou et al. 2020). Overall, soil pH was higher in GL than in RP, and a higher pH promoted bacterial growth (Xu et al. 2022). Then led to an increase in bacterial residues. Compared to woody plants, herbaceous plants have a relatively low lignin content, and enzymes produced in bacteria readily degrade substrates at a faster rate (Cotrufo et al. 2013). Therefore, bacterial residues are synthesized in the soil at a greater rate and make a greater contribution than fungal residues (Huang et al. 2021). The carbon content of fungal residues in RP contributed more (17.4–33.3%) to SOC (Fig. 3). Given the mulching effect of litter on the soil (Table 1), which

reduces the disturbance of the soil by the external environment, the mycelia of the fungus are retained (Wang et al. 2021). This, coupled with the fact that the difficult to decompose components of the litter can be better used by fungi, accelerates their growth and metabolites, and contributes to fungal residues in RP more significantly (Zhao et al. 2023).

Different contributions of plant and microbial residual carbon to SOC changed with the recovery years

With the increasing restoration years, the aboveground biomass in GL and RP, as well as that of litter biomass, accumulated (Table 1). This has provided more carbon and nutrients for root growth, and the increase in root exudates stimulated the growth of microorganisms (Canto et al. 2020), further increasing the amounts of microbial residues and their contribution to SOC (Fig. 5). In addition, the microbial entombing effect increases the accumulation of microbial residues and promotes the formation of stable organic carbon in soil through microbial in vivo turnover (Han et al. 2024; Wu et al. 2024). Meanwhile, the increase in soil water content led to an increase in microbial activity and a more rapid rate of plant residue decomposition (Table 2), resulting in a decrease in plant residue content. The enhancement of microbial activity was accompanied by a rise in the number of microorganisms and, consequently, an increase in the content of microbial residues, which increased the contribution to SOC (Xue et al. 2024). Catalase can depolymerize lignin while cellobiohydrolase can degrade cellulose, both provide readily available substrates for microorganisms to use (Chen et al. 2021; Meng et al. 2022; Zhang et al. 2019). This facilitates the accumulation of microbial residues while reducing the accumulation of plant residue carbon. Next, (Ac-to-Al)_v and (Ac-to-Al)_s reflect the degree of microbial oxidation of side chains (Sokol et al. 2019)_d and S/V reflect the degree of decomposition of plant residue carbon (Chen et al. 2021). The results of this study verify that the (Ac-to-Al)_v and (Ac-to-Al)_s values of GL and RP tended to increase, and the C/V and S/V values tended to decrease with increasing restoration years (Fig. S2). This has indicated an increase in the level of microbial oxidative decomposition, a decrease in the concentration of lignin phenols, and an increase in the decomposition



◀**Fig. 5** Redundancy analysis showed the effects of vegetation characteristics and soil physicochemical properties on residual carbon and its contribution to soil organic carbon under different vegetation types. Note: (a) and (e): the relationships between residual carbon content, its contribution to soil organic carbon (blue arrows) and vegetation characteristics (red arrows); (c) and (g): the relationships between residual carbon content, its contribution to soil organic carbon (blue arrow) and soil characteristics (red arrow). LB: little biomass, LC: little carbon content, LN: little nitrogen content, FRB: fine root biomass, FRC: fine root carbon content, FRN: fine root nitrogen content, FRC/N: fine root carbon–nitrogen ratio, PC/N: plant carbon–nitrogen ratio, BD: Soil bulk density, SWC: soil water content, MBC/MBN: microbial biomass carbon–nitrogen ratio, SOC: soil organic carbon, Soil C/N: soil organic carbon–total nitrogen ratio, P-contribute: contribution of plant residue carbon to soil organic carbon, M-contribute: contribution of microbial residue carbon to soil organic carbon, B-contribute: contribution of bacterial residue carbon to soil organic carbon, F-contribute: contribution of fungal residue carbon to soil organic carbon, P-C: plant residue carbon content, M-C: microbial residue carbon content, B-C: bacterial residue carbon content, FC: fungal residue carbon content. Treatment codes are the same as Fig. 1

of plant residue carbon (Yang et al. 2022a). The interaction of clay with amino compounds has a significant effect on amino sugar stability and clay is the main storage reservoir for microbial residue accumulation (Hu and Lan 2020; Wang et al. 2022b). The increasing of clay content further enhanced the stability of microbial residues with an increased contribution. (Table 1).

Different contributions of bacterial and fungal residual carbon to SOC changed with the recovery years

In GL and RP restorations, the relative contribution of bacterial residue C decreased, and the relative contribution of fungal residue carbon increased (Fig. 3). With the increasing restoration years, the soil pH in GL and RP gradually decreased, bacterial growth was gradually suppressed, and the number of fungal residues increased (Xu et al. 2022). Furthermore, soil clay plays a protective role in the stabilization of microbial residues, and especially fungal residues (Wang et al. 2022b). Clay may improve the substrate access to fungi during the vegetation restoration, thus enhancing their hyphal proliferation (Li et al. 2024a). Moreover, it has been shown that the clay content is significantly correlated with the content of microaggregates (Abid et al. 2018), and the small pore size of microaggregates

hinders the contact between fungal residue carbon and extracellular enzymes, and slows down the decomposition of fungal residue carbon (Wang et al. 2022b). Therefore, the content of fungal residue carbon is higher in soils with higher clay content during the restoration (Table 2). What's more, the different contributions of bacterial and fungal residual carbon to SOC with increasing restoration years was also due to their different life history responses (Zhang et al. 2016). Most bacteria, such as Actinobacteria and Proteobacteria, are usually classified as r-strategists, which have a fast growth rate due to their rapid response to effective nutrient inputs (Yang et al. 2022b). Thus, bacteria residues carbon played a dominant role in the accumulation of SOC in the early stages of vegetation restoration (Fig. 3a, b, c). In contrast, most fungi, such as Basidiomycota and ectomycorrhizal fungi, are typically classified as k-strategists and have a longer life cycle (Li et al. 2021b). Therefore, fungal residues carbon was crucial for the contribution of SOC in the later stages of vegetation restoration (Fig. 3). Also, bacteria have thin cell walls that are easily broken down, whereas fungal cell polymers are relatively stable and thus preserved in SOC in the later stage of vegetation restoration (Xu et al. 2022). However, our results are inconsistent with the research in the Yunwu Mountain Nature Reserve, which found that the contribution of bacterial residues to SOC increased with recovery years and was over than that of fungal residues by (Yang et al. 2022a). The reason for this difference may be that the microbial carbon content of the Yunwu Mountain Nature Reserve soil was higher than that after grassland restoration in this study, in which the biomass of living bacteria was greater than that of fungi. Therefore, bacterial residues contributed more to the SOC (Guo et al. 2021). The soil carbon–nitrogen ratio in this study was relatively high, and bacterial growth is more easily limited by nitrogen (Wang et al. 2021), so the results obtained in this study indicated a larger contribution of fungal residue carbon.

The accumulation of SOC mediated by plants, fungi, and bacteria under different vegetation types

Fungal and bacterial residue carbon were more closely correlated with GL, whereas fungal and plant residue carbon were more strongly correlated with RP (Fig. 6). This result may be ascribed to the following reasons: First, the litter and foliage

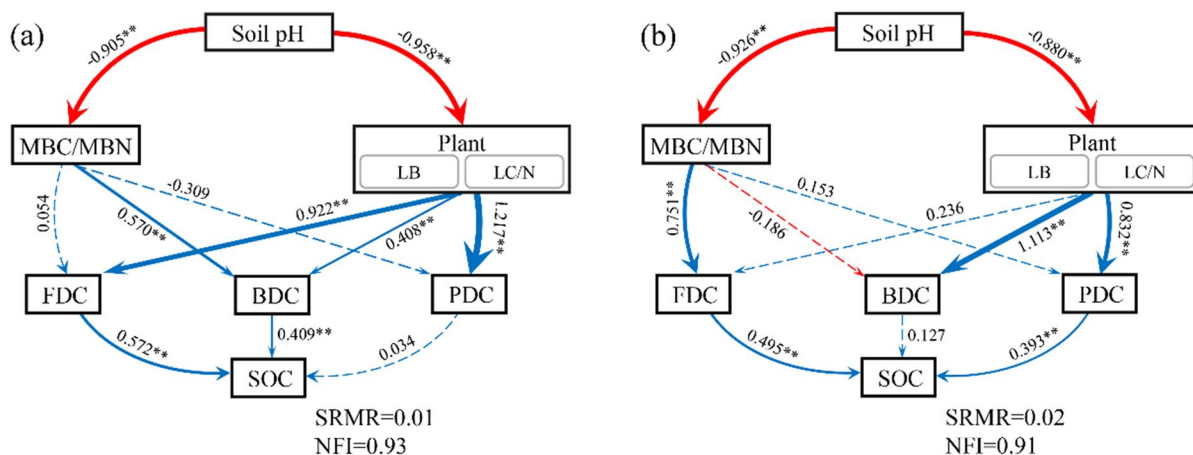


Fig. 6 Partial least squares path model revealing the direct and indirect effects of plant, fungal, and bacterial residue carbon contents on soil organic carbon in grasslands (a) and *Robinia pseudoacacia* plantations (b). Note: MBC/MBN: microbial biomass carbon–nitrogen ratio, LB: litter biomass, LC/LN: litter biomass carbon–nitrogen ratio, FDC: fungal residue carbon,

BDC: bacterial residue carbon, PDC: plant residue carbon, SOC: soil organic carbon. The standardized path coefficient is listed on the path in the figure, the thickness of the arrow indicates the path coefficient, the blue represents positive effects, red represents negative effects, ** $P < 0.01$

inputs in RP were substantially higher than those in GL (Table 1), and the higher aboveground carbon input and lower belowground carbon input were unfavorable for microbial anabolism and microbial residue accumulation (Dai et al. 2022). Therefore, the contribution of plant residue carbon to the SOC in RP was higher. Second, the lower pH of the RP may have inhibited microbial activity compared with that of the GL, affecting the accumulation of microbial residues (Angst et al. 2021). Fungal residue carbon had a significant effect on SOC in both GL and RP. With the increase of recovery years, difficult to degrade materials such as cellulose and lignin gradually increased. The role of fungi gradually became apparent because fungi can use more recalcitrant components as nutrients than bacteria (Zhang et al. 2024). This phenomenon may also be related to the composition of the microbial cell wall. The main chemical component of the bacterial cell wall is peptidoglycan, which can be broken down into peptides and directly used by microorganisms. The fungal cell wall is mainly composed of chitin, a more stable compound that can be retained in the soil for a longer period (Coonan et al. 2020). Therefore, the degradation of fungal residues is slower (Fernandez et al. 2016; Jones et al. 2019) and has a greater impact on SOC.

Conclusion

Vegetation restoration can improve the physicochemical properties of soil and contribute to the accumulation and retention of SOC, in which plant and microbial residues play a key role. With increasing recovery years, the content of plant and microbial residues increased, but their contributions to SOC decreased and increased, respectively. More organic carbon accumulated in GL and RP in the form of microbial and plant residue carbon, respectively. The content of bacterial and fungal residues both showed an increasing trend. However, their contribution to SOC showed different trends. The relative contribution of bacterial residue C decreased, and the relative contribution of fungal residue carbon increased. With an increase in recovery years, the largest relative microbial contributions to SOC in GL changed from bacterial residue carbon to fungal residue carbon. However, RP was dominated by fungal residue carbon. Taken together, these results have highlighted the contribution of plant and microbial residues to SOC during vegetation restoration, more effectively elucidating the role of plants and microorganisms in SOC sequestration. Our research not only contributes to understanding the complexity of the carbon cycle in ecosystems, but also provides valuable scientific evidence for adopting differentiated strategies to manage and conserve soil resources under various vegetation types.

Acknowledgements This work was supported by the Forestry Science and Technology Innovation Project of Shaanxi Province [No. SXLK2022-02-14]; Key Research and Development Projects of Shaanxi Province [No. 2022SF-285]; the National Natural Science Foundation of China [No. 42007428]; and the Chinese Universities Scientific Fund [2452023079].

Declarations

Conflict of interest No conflict of interest exists in the submission of this manuscript, and manuscript is approved by all authors for publication. I would like to declare on behalf of my co-authors that the work described was original research that has not been published previously, and not under consideration for publication elsewhere, in whole or in part.

References

- Abid Y, Casillo A, Gharsallah H, Joulak I, Lanzetta R, Corsaro MM, Attia H, Azabou S (2018) Production and structural characterization of exopolysaccharides from newly isolated probiotic lactic acid bacteria. *Int J Biol Macromol* 108:719–728. <https://doi.org/10.1016/j.ijbiomac.2017.10.155>
- Angst G, Mueller KE, Nierop KGJ, Simpson MJ (2021) Plant- or microbial-derived? A review on the molecular composition of stabilized soil organic matter. *Soil Biol Biochem* 156:108189. <https://doi.org/10.1016/j.soilbio.2021.108189>
- Arcidiacono M, Pellegrino E, Nuti M, Ercoli L (2023) Field inoculation by arbuscular mycorrhizal fungi with contrasting life-history strategies differently affects tomato nutrient uptake and residue decomposition dynamics. *Plant Soil*. <https://doi.org/10.1007/s11104-023-05995-8>
- Beidler K, Phillips RP, Andrews E, Maillard F, Mushinski RM, Kennedy PG (2020) Substrate quality drives fungal necromass decay and decomposer community structure under contrasting vegetation types. *J Ecol* 108:1845–1859. <https://doi.org/10.1111/1365-2745.13385>
- Canto CD, Simonin M, King E, Moulin L, Bennett MJ, Castrillo G, Laplaze L (2020) An extended root phenotype: the rhizosphere, its formation and impacts on plant fitness. *Plant J* 103:951–964. <https://doi.org/10.1111/tj.14781>
- Cao L, Xu MP, Liu YS, Yu ZC, Sun L, Tian XF, Zhang Y, Shi JY, Han XH, Yang PZ, Zhang W (2023) Response of soil nitrogen components and its vertical distribution to rain-fall redistribution during *Robinia pseudoacacia* forest restoration on the Loess Plateau. *Ecol Indic* 155:111036. <https://doi.org/10.1016/j.ecolind.2023.111036>
- Charles SP, Kominoski JS, Armitage AR, Guo HY, Weaver CA, Pennings SC (2020) Quantifying how changing mangrove cover affects ecosystem carbon storage in coastal wetlands. *Ecology* 101:e02916. <https://doi.org/10.1002/ecy.2916>
- Chen XB, Hu YJ, Xia YH, Zheng SM, Ma C, Rui YC, He HB, Huang DY, Zhang ZH, Ge TD, Wu JS, Guggenberger G, Kuzyakov Y, Su YR (2021) Contrasting pathways of carbon sequestration in paddy and upland soils. *Global Change Biol* 27:2478–2490. <https://doi.org/10.1111/gcb.15595>
- Cheng JM, Zhao MX, Cong J, Qi Q, Xiao Y, Cong W, Deng Y, Zhou JZ, Zhang YG (2020) Soil pH exerts stronger impacts than vegetation type and plant diversity on soil bacterial community composition in subtropical broad-leaved forests. *Plant Soil* 450:273–286. <https://doi.org/10.1007/s11104-020-04507-2>
- Coonan EC, Kirkby CA, Kirkegaard JA, Amidy MR, Strong CL, Richardson AE (2020) Microorganisms and nutrient stoichiometry as mediators of soil organic matter dynamics. *Nutr Cycl Agroecosys* 117:273–298. <https://doi.org/10.1007/s10705-020-10076-8>
- Cotrufo MF, Wallenstein MD, Boot CM, Deneff K, Paul E (2013) The Microbial Efficiency-Matrix stabilization (MEMS) framework integrates plant litter decomposition with soil organic matter stabilization: do labile plant inputs form stable soil organic matter? *Global Change Biol* 19:988–995. <https://doi.org/10.1111/gcb.12113>
- Dai GH, Zhu SS, Cai Y, Zhu ER, Jia YF, Ji CJ, Tang ZY, Fang JY, Feng XJ (2022) Plant-derived lipids play a crucial role in forest soil carbon accumulation. *Soil Biol Biochem* 168:108645. <https://doi.org/10.1016/j.soilbio.2022.108645>
- DeForest JL (2009) The influence of time, storage temperature, and substrate age on potential soil enzyme activity in acidic forest soils using MUB-linked substrates and L-DOPA. *Soil Biol Biochem* 41:1180–1186. <https://doi.org/10.1016/j.soilbio.2009.02.029>
- Deng L, Liu GB, Shangguan ZP (2014) Land-use conversion and changing soil carbon stocks in China's 'Grain-for-Green' program: a synthesis. *Glob Chang Biol* 20:3544–3556. <https://doi.org/10.1111/gcb.12508>
- Ding XL, Chen SY, Zhang B, He HB, Filley TR, Horwath WR (2020) Warming yields distinct accumulation patterns of microbial residues in dry and wet alpine grasslands on the Qinghai-Tibetan Plateau. *Biol Fertil Soils* 56:881–892. <https://doi.org/10.1007/s00374-020-01474-9>
- Feng ZW, Liu XD, Qin YQ, Feng GD, Zhou Y, Zhu HH, Yao Q (2023) Cooperation of arbuscular mycorrhizal fungi and bacteria to facilitate the host plant growth dependent on soil pH. *Front Microbiol* 14:1116943. <https://doi.org/10.3389/fmicb.2023.1116943>
- Fernandez CW, Langley JA, Chapman S, McCormack ML, Koide RT (2016) The decomposition of ectomycorrhizal fungal necromass. *Soil Biol Biochem* 93:38–49. <https://doi.org/10.1016/j.soilbio.2015.10.017>
- Ghani MI, Wang J, Li P, Pathan SI, Sial TA, Datta R, Mokhtar A, Ali EF, Rinklebe J, Shaheen SM, Liu MY, Abdelrahman H (2023) Variations of soil organic carbon fractions in response to conservative vegetation successions on the Loess Plateau of China. *Int Soil Water Conserv Res* 11:561–571. <https://doi.org/10.1016/j.iswcr.2022.05.002>
- Guo ZM, Zhang XY, Dunggait JAJ, Green SM, Wen XF, Quine TA (2021) Contribution of soil microbial necromass to SOC stocks during vegetation recovery in a subtropical karst ecosystem. *Sci Total Environ* 761:143945. <https://doi.org/10.1016/j.scitotenv.2020.143945>
- Han BB, Yao YZ, Wang YN, Su XX, Ma LH, Chen XP, Li ZL (2024) Microbial traits dictate soil necromass

- accumulation coefficient: a global synthesis. *Global Ecol Biogeogr* 33:151–161. <https://doi.org/10.1111/gcb.13776>
- Hao XX, Han XZ, Wang C, Yan J, Lu XC, Chen X, Zou WX (2023) Temporal dynamics of density separated soil organic carbon pools as revealed by $\delta^{13}\text{C}$ changes under 17 years of straw return. *Agric Ecosyst Environ* 356:108656. <https://doi.org/10.1016/j.agee.2023.108656>
- He M, Fang K, Chen LY, Feng XH, Qin SQ, Kou D, He HB, Liang C, Yang YH (2022) Depth-dependent drivers of soil microbial necromass carbon across tibetan alpine grasslands. *Glob Chang Biol* 28:936–949. <https://doi.org/10.1111/gcb.15969>
- Hedges JJ, Ertel JR (1982) Characterization of lignin by gas capillary chromatography of cupric oxide oxidation products. *Anal Chem* 54:174–178. <https://doi.org/10.1021/ac00239a007>
- Hu N, Lan JC (2020) Impact of vegetation restoration on soil organic carbon stocks and aggregates in a karst rocky desertification area in Southwest China. *J Soils Sediments* 20:1264–1275. <https://doi.org/10.1007/s11368-019-02532-y>
- Huang RL, Crowther TW, Sui YY, Sun B, Liang YT (2021) High stability and metabolic capacity of bacterial community promote the rapid reduction of easily decomposing carbon in soil. *Commun Biol* 4:1376. <https://doi.org/10.1038/s42003-021-02907-3>
- Joergensen RG (2018) Amino sugars as specific indices for fungal and bacterial residues in soil. *Biol Fert Soil* 54:559–568. <https://doi.org/10.1007/s00374-018-1288-3>
- Jones DL, Cooledge EC, Hoyle FC, Griffiths RI, Murphy DV (2019) pH and exchangeable aluminum are major regulators of microbial energy flow and carbon use efficiency in soil microbial communities. *Soil Biol Biochem* 138:107584. <https://doi.org/10.1016/j.soilbio.2019.107584>
- Li J, Sang CP, Yang JY, Qu LR, Xia ZW, Sun H, Jiang P, Wang XG, He HB, Wang C (2021a) Stoichiometric imbalance and microbial community regulate microbial elements use efficiencies under nitrogen addition. *Soil Biol Biochem* 156:108207. <https://doi.org/10.1016/j.soilbio.2021.108207>
- Li H, Yang S, Semenov MV, Yao F, Ye J, Bu RC, Ma R, Lin JJ, Kurganova I, Wang XG, Deng Y, Kravchenko I, Jiang Y, Kuzyakov Y (2021b) Temperature sensitivity of SOM decomposition is linked with a K-selected microbial community. *Glob Change Biol* 27:2763–2779. <https://doi.org/10.1111/gcb.15593>
- Li Y, Zhang W, Li J, Zhou F, Liang XA, Zhu XF, He HB, Zhang XD (2023) Complementation between microbial necromass and plant debris governs the long-term buildup of the soil organic carbon pool in conservation agriculture. *Soil Biol Biochem* 178:108963. <https://doi.org/10.1016/j.soilbio.2023.108963>
- Li YZ, Bao XL, Tang SX, Xiao KQ, Ge CJ, Xie HT, He HB, Mueller CW, Liang C (2024a) Toward soil carbon storage: the influence of parent material and vegetation on profile-scale microbial community structure and necromass accumulation. *Soil Biol Biochem* 193:109399. <https://doi.org/10.1016/j.soilbio.2024.109399>
- Li YH, Xiao ML, Wei L, Liu Q, Zhu ZK, Yuan HZ, Wu JS, Yuan J, Wu XH, Kuzyakov Y, Ge TD (2024b) Bacterial necromass determines the response of mineral-associated organic matter to elevated CO₂. *Biol Fert Soils* 60:327–340. <https://doi.org/10.1007/s00374-024-01803-2>
- Liang C, Amelung W, Lehmann J, Kastner M (2019) Quantitative assessment of microbial necromass contribution to soil organic matter. *Glob Chang Biol* 25:3578–3590. <https://doi.org/10.1111/gcb.14781>
- Liang C, Zhu XF (2021) The soil microbial carbon pump as a new concept for terrestrial carbon sequestration. *Sci China Earth Sci* 64:545–558. <https://doi.org/10.1007/s11430-020-9705-9>
- Ma T, Zhu SS, Wang ZH, Chen DM, Dai GH, Feng BW, Su XY, Hu HF, Li KH, Han WX, Liang C, Bai YF, Feng XJ (2018) Divergent accumulation of microbial necromass and plant lignin components in grassland soils. *Commun* 9:3480. <https://doi.org/10.1038/s41467-018-05891-1>
- Medeiros AD, Cesario FV, Maia SMF (2023) Long-term impact of conventional management on soil carbon and nitrogen stocks in the semi-arid region of Brazil: a meta-analysis. *J Arid Environ* 218:105052. <https://doi.org/10.1016/j.jaridenv.2023.105052>
- Meng LX, Xu CX, Wu FL, Huhe (2022) Microbial co-occurrence networks driven by low-abundance microbial taxa during composting dominate lignocellulose degradation. *Sci Total Environ* 845:157197. <https://doi.org/10.1016/j.scitotenv.2022.157197>
- Qian ZY, Li YN, Du H, Wang KL, Li DJ (2023) Increasing plant species diversity enhances microbial necromass carbon content but does not alter its contribution to soil organic carbon pool in a subtropical forest. *Soil Biol Biochem* 187:109183. <https://doi.org/10.1016/j.soilbio.2023.109183>
- Qin GM, He WJ, Sanders CJ, Zhang JF, Zhou JE, Wu JT, Lu Z, Yu MX, Li YW, Li YX, Lambers H, Li Z, Wang FM (2024) Contributions of plant- and microbial-derived residuals to mangrove soil carbon stocks: implications for blue carbon sequestration. *Funct Ecol* 38:573–585. <https://doi.org/10.1111/1365-2435.14497>
- Roth VN, Lange M, Simon C, Hertkorn N, Bucher S, Goodall T, Griffiths RI, Mellado-Vázquez PG, Mommer L, Oram NJ, Weigelt A, Dittmar T, Gleixner G (2019) Persistence of dissolved organic matter explained by molecular changes during its passage through soil. *Nat Geosci* 12:755. <https://doi.org/10.1038/s41561-019-0417-4>
- Saiya-Cork KR, Sinsabaugh RL, Zak DR (2002) The effects of long term nitrogen deposition on extracellular enzyme activity in an *Acer saccharum* forest soil. *Soil Biol Biochem* 34:1309–1315. [https://doi.org/10.1016/S0038-0717\(02\)00074-3](https://doi.org/10.1016/S0038-0717(02)00074-3)
- Sokol NW, Sanderman J, Bradford MA (2019) Pathways of mineral-associated soil organic matter formation: integrating the role of plant carbon source, chemistry, and point of entry. *Glob Chang Biol* 25:12–24. <https://doi.org/10.1111/gcb.14482>
- Sun L, Yu ZC, Tian XF, Zhang Y, Shi JY, Fu R, Liang YJ, Zhang W (2023) Leguminosae plants play a key role in affecting soil physical-chemical and biological properties during grassland succession after farmland abandonment in the Loess Plateau, China. *J Arid Land* 15:1107–1128. <https://doi.org/10.1007/s40333-023-0025-4>
- Tian XF, Zhang Y, Liang YJ, Fu R, Sun L, Yu ZC, Shi JY, Sailike A, Hao HJ, Zhang W (2024) Differential response of soil bacteria and fungi to carbon and respiration components in abandoned grasslands on the

- Loess Plateau, China. *Plant Soil*. <https://doi.org/10.1007/s11104-024-06628-4>
- Tian P, Zhao XC, Liu SG, Wang QG, Zhang W, Guo P, Razavi BS, Liang C, Wang QK (2022) Differential responses of fungal and bacterial necromass accumulation in soil to nitrogen deposition in relation to deposition rate. *Sci Total Environ* 847:157645. <https://doi.org/10.1016/j.scitotenv.2022.157645>
- Voosen P (2022) Hot' climate models exaggerate Earth impacts. *Science* 376:685–685. <https://doi.org/10.1126/science.adc9453>
- Wang BR, An SS, Liang C, Liu Y, Kuzyakov Y (2021) Microbial necromass as the source of soil organic carbon in global ecosystems. *Soil Biol Biochem* 162:108422. <https://doi.org/10.1016/j.soilbio.2021.108422>
- Wang MM, Guo XW, Zhang S, Xiao LJ, Mishra U, Yang YH, Zhu BA, Wang GC, Mao XL, Qian T, Jiang T, Shi Z, Luo ZK (2022a) Global soil profiles indicate depth-dependent soil carbon losses under a warmer climate. *Nat Commun* 13:5514. <https://doi.org/10.1038/s41467-022-33278-w>
- Wang BR, Huang YM, Li N, Yao HJ, Yang E, Soromotin AV, Kuzyakov Y, Cheptsov V, Yang Y, An SS (2022b) Initial soil formation by biocrusts: Nitrogen demand and clay protection control microbial necromass accrual and recycling. *Soil Biol Biochem* 167:108607. <https://doi.org/10.1016/j.soilbio.2022.108607>
- Wang X, Wang Z, Chen F, Zhang Z, Fang J, Xing L, Zeng J, Zhang Q, Liu H, Liu W, Ren C, Yang G, Zhong Z, Zhang W, Han X (2024) Deterministic assembly of grassland soil microbial communities driven by climate warming amplifies soil carbon loss. *Sci Total Environ* 923:171418. <https://doi.org/10.1016/j.scitotenv.2024.171418>
- Wu HW, Cui HL, Fu CX, Li R, Qi FY, Liu ZL, Yang G, Xiao KQ, Qiao M (2024) Unveiling the crucial role of soil microorganisms in carbon cycling: a review. *Sci Total Environ* 909:168627. <https://doi.org/10.1016/j.scitotenv.2023.168627>
- Xiang XJ, Gibbons SM, Li H, Shen HH, Fang JY, Chu HY (2018) Shrub encroachment is associated with changes in soil bacterial community composition in a temperate grassland ecosystem. *Plant Soil* 425:539–551. <https://doi.org/10.1007/s11104-018-3605-x>
- Xiao KQ, Zhao Y, Liang C, Zhao MY, Moore OW, Otero-Fariña A, Zhu YG, Johnson K, Peacock CL (2023) Introducing the soil mineral carbon pump. *Nat Rev Earth Environ* 4:135–136. <https://doi.org/10.1038/s43017-023-00396-y>
- Xu YD, Gao XD, Liu YL, Li SY, Liang C, Lal R, Wang JK (2022) Differential accumulation patterns of microbial necromass induced by maize root vs. shoot residue addition in agricultural Alfisols. *Soil Biol Biochem* 164:108474. <https://doi.org/10.1016/j.soilbio.2021.108474>
- Xu YD, Wang T, Li H, Ren CJ, Chen JW, Yang GH, Han XH, Feng YZ, Ren GX, Wang XJ (2019) Variations of soil nitrogen-fixing microorganism communities and nitrogen fractions in a Robinia pseudoacacia chronosequence on the Loess Plateau of China. *Catena* 174:316–323. <https://doi.org/10.1016/j.catena.2018.11.009>
- Xue ZJ, Qu TT, Li XY, Chen Q, Zhou ZC, Wang BR, Lv XZ (2024) Different contributing processes in bacterial vs. fungal necromass affect soil carbon fractions during plant residue transformation. *Plant Soil* 494:301–319. <https://doi.org/10.1007/s11104-023-06277-z>
- Xue YH, Zhao FY, Sun ZX, Bai W, Zhang YY, Zhang Z, Yang N, Feng C, Feng LS (2023) Long-term mulching of biodegradable plastic film decreased fungal necromass C with potential consequences for soil C storage. *Chemosphere* 337:139280. <https://doi.org/10.1016/j.chemosphere.2023.139280>
- Yang Y, Dou YX, Wang BR, Wang YQ, Liang C, An SS, Soromotin A, Kuzyakov Y (2022a) Increasing contribution of microbial residues to soil organic carbon in grassland restoration chronosequence. *Soil Biol Biochem* 170:108688. <https://doi.org/10.1016/j.soilbio.2022.108688>
- Yang Y, Dou YX, Wang BR, Xue ZJ, Wang YQ, An SS, Chang SX (2022b) Deciphering factors driving soil microbial life-history strategies in restored grasslands. *iMeta* 2:e66. <https://doi.org/10.1002/IMT2.66>
- Yang Y, Liu H, Yang X, Yao HJ, Deng XQ, Wang YQ, An SS, Kuzyakov Y, Chang SX (2022c) Plant and soil elemental C:N:P ratios are linked to soil microbial diversity during grassland restoration on the Loess Plateau, China. *Sci Total Environ* 806:150557. <https://doi.org/10.1016/j.scitotenv.2021.150557>
- Yang YL, Xie HT, Mao Z, Bao XL, He HB, Zhang XD, Liang C (2022d) Fungi determine increased soil organic carbon more than bacteria through their necromass inputs in conservation tillage croplands. *Soil Biol Biochem* 167:108587. <https://doi.org/10.1016/j.soilbio.2022.108587>
- Yang Y, Sun H, Zhang PP, Wu F, Qiao JB, Li TC, Wang YQ, An SS (2023) Review of managing soil organic C sequestration from vegetation restoration on the Loess Plateau. *Forests* 14:1964. <https://doi.org/10.3390/f14101964>
- Ye LP, Ji LL, Chen HF, Chen XY, Tan WF (2022) Spatial contribution of environmental factors to Soil Aggregate Stability in a small catchment of the Loess Plateau, China. *Agronomy-Basel* 12:2557. <https://doi.org/10.3390/agronomy12102557>
- Yuan ZQ, Song X, Feng ZZ, Wang J, Wang RZ, Agathokleous E, Fang C, Sardans J, Penuelas J (2023) Soil organic carbon and nitrogen sequestration following grazing exclusion on the Loess Plateau, China. *Catena* 232:107412. <https://doi.org/10.1016/j.catena.2023.107412>
- Zeng XM, Feng J, Yu DL, Wen SH, Zhang QG, Huang QY, Delgado-Baquerizo M, Liu YR (2022) Local temperature increases reduce soil microbial residues and carbon stocks. *Glob Chang Biol* 28:6433–6445. <https://doi.org/10.1111/gcb.16347>
- Zhang XD, Amelung W (1996) Gas chromatographic determination of muramic acid, glucosamine, mannosamine, and galactosamine in soils. *Soil Biol Biochem* 28:1201–1206. [https://doi.org/10.1016/0038-0717\(96\)00117-4](https://doi.org/10.1016/0038-0717(96)00117-4)
- Zhang C, Liu GB, Xue S, Wang GL (2016) Soil bacterial community dynamics reflect changes in plant community and soil properties during the secondary succession of abandoned farmland in the Loess Plateau. *Soil Biol Biochem* 97:40–49. <https://doi.org/10.1016/j.soilbio.2016.02.013>
- Zhang Q, Li XY, Liu JJ, Liu JY, Han L, Wang X, Liu HY, Xu MP, Yang GH, Ren CJ, Han XH (2023a) The contribution of microbial necromass carbon to soil organic carbon in soil aggregates. *Appl Soil Ecol* 190:104985. <https://doi.org/10.1016/j.apsoil.2023.104985>

- Zhang JF, Zhou JG, Sayer EJ, Lambers H, Liu ZF, Lu XK, Li YW, Li YX, Li H, Wang FM (2023b) Nitrogen deposition enhances soil organic carbon and microbial residual carbon in a tropical forest. *Plant Soil* 484:217–235. <https://doi.org/10.1007/s11104-022-05787-6>
- Zhang XX, Song JX, Wang YR, Sun HT, Li Q (2022) Threshold effects of vegetation coverage on runoff and soil loss in the Loess Plateau of China: a meta-analysis. *Geoderma* 412:115720. <https://doi.org/10.1016/j.geoderma.2022.115720>
- Zhang Y, Chen YP, An B, Ma XQ, Zhang H, Liu QG, Mao R (2024) The succession patterns and drivers of soil bacterial and fungal communities with stand development in Chinese fir plantations. *Plant Soil*. <https://doi.org/10.1007/s11104-024-06502-3>
- Zhang W, Xu YD, Gao DX, Wang X, Liu WC, Deng J, Han XH, Yang GH, Feng YZ, Ren GX (2019) Ecoenzymatic stoichiometry and nutrient dynamics along a revegetation chronosequence in the soils of abandoned land and plantation on the Loess Plateau, China. *Soil Biol Biochem* 134:1–14. <https://doi.org/10.1016/j.soilbio.2019.03.017>
- Zhao XC, Tian P, Liu SG, Yin P, Sun ZL, Wang QK (2023) Mean annual temperature and carbon availability respectively controlled the contributions of bacterial and fungal residues to organic carbon accumulation in topsoil across China's forests. *Glob Ecol Biogeogr* 32:120–131. <https://doi.org/10.1111/geb.13605>
- Zhou RR, Liu Y, Dungait JAJ, Kumar A, Wang JS, Tiemann LK, Zhang FS, Kuzyakov Y, Tian J (2023) Microbial necromass in cropland soils: a global meta-analysis of management effects. *Glob Change Biol* 29:1998–2014. <https://doi.org/10.1111/gcb.16613>
- Zhou ZH, Wang CK, Luo YQ (2020) Meta-analysis of the impacts of global change factors on soil microbial diversity and functionality. *Nat Commun* 11:3072. <https://doi.org/10.1038/s41467-020-16881-7>

Publisher's Note Springer Nature remains neutral with regard to jurisdictional claims in published maps and institutional affiliations.

Springer Nature or its licensor (e.g. a society or other partner) holds exclusive rights to this article under a publishing agreement with the author(s) or other rightsholder(s); author self-archiving of the accepted manuscript version of this article is solely governed by the terms of such publishing agreement and applicable law.